Mesoscopic Josephson effect

HERMANN GRABERT
Fakultät für Physik, Albert-Ludwigs-Universität, Hermann-Herder-Straße 3, D-79104 Freiburg, Germany

GERT-LUDWIG INGOLD
Institut für Physik, Universität Augsburg, Universitätsstraße 1, D-86135 Augsburg, Germany
CEA, Service de Physique de l'Etat Condensé, Centre d'Etudes de Saclay, F-91191 Gif-sur-Yvette, France

1. Introduction

The Josephson effect beautifully embodies quantum tunneling and superconductivity [1, 2]. Josephson systems have been a subject of fundamental research for decades, which have led to useful applications, e.g. in highly sensitive magnetometry and metrology. Like in the Ginzburg–Landau theory for bulk superconductivity, where the phase of the order parameter is considered as a quasiclassical variable, the phase difference across a Josephson junction can frequently be treated classically. However, in the last ten years or so, new lithography and low-temperature techniques have allowed the fabrication and measurement of small Josephson junctions affected by the capacitive charging energy of single Cooper pairs [3, 4]. A large charging energy will render the Cooper pair number on either side of the junction classical and, thus, cause large quantum fluctuations of the conjugate phase variable.

In this article we show how the classical Josephson effect, that is a supercurrent I flowing at vanishing voltage V, gradually evolves via the classical phase diffusion regime into the supercurrent peak in the Coulomb blockade regime, where Cooper pairs tunnel incoherently across the Josephson junction. After a brief review of the classical Josephson effect in Section 2 and phase diffusion in Section 3, we discuss Cooper pair tunneling in the Coulomb blockade regime in Section 4. The turnover between the classical and the quantum regimes is discussed in Section 5. Finally, Section 6 contains some concluding remarks.

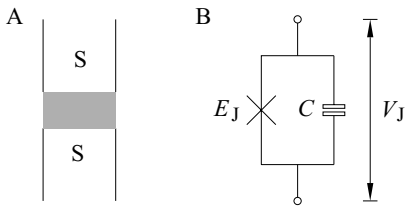

Fig. 1. A, Schematic view of a Josephson junction where two superconductors are separated by an insulating barrier. B, Equivalent circuit with Josephson coupling E_J and capacitance C. The voltage across the junction is denoted by V_J.

2. Classical Josephson effect

A Josephson junction consists of two superconductors separated by a thin insulating barrier as shown in Fig. 1A. Its dynamics may be described in terms of the phase difference φ of the two condensate wavefunctions on the left and right sides of the junction and the number n of Cooper pairs on the capacitor formed by the junction. These operators n and φ obey the commutation relation $[n, \varphi] = -i$, and the junction Hamiltonian may be expressed as

$$H_J = E_c n^2 - E_J \cos(\varphi). \tag{1}$$

The first term describes the charging energy associated with the capacitance C of the tunnel junction where $E_c = 2e^2/C$ is the charging energy corresponding to a single Cooper pair. The second term arises from the tunneling of Cooper pairs through the junction characterized by the Josephson coupling energy E_J. These properties may be expressed in terms of the circuit shown in Fig. 1B.

The Josephson relations link the phase to the voltage across the junction

$$V_J = \frac{\hbar}{2e}\dot{\varphi} \tag{2}$$

and to the supercurrent

$$I = I_c \sin(\varphi). \tag{3}$$

The critical current I_c is related to the Josephson coupling energy by $I_c = 2eE_J/\hbar$. These relations allow for a supercurrent flowing at zero voltage if φ remains constant in time.

3. Phase diffusion in Josephson junctions

In the real world Josephson junctions are coupled to an electromagnetic environment which may be described by an impedance $Z(\omega)$. For simplicity, we will in the following mostly consider the case of an ohmic resistor [$Z(\omega) = R$] but a more general case will be addressed in Section 4. The resistor will give rise to Nyquist noise and therefore to a diffusive behavior of the phase difference φ.

To be specific, we consider the circuit shown in Fig. 2 where the Josephson junction is coupled to the voltage source via an ohmic resistor. The voltages across the junction and the resistor are denoted by V_J and V_R, respectively. It is useful to introduce the dimensionless resistance $\rho = R/R_Q$, where $R_Q = h/4e^2$ is the resistance quantum for Cooper pairs.

In the classical limit this system can be described by the Langevin equation [1, 5]

$$C\left(\frac{\hbar\ddot{\varphi}}{2e} + \frac{1}{R}\frac{\hbar\dot{\varphi}}{2e} + I_c \sin(\varphi) = \frac{V_R}{R}.\right. \tag{4}$$

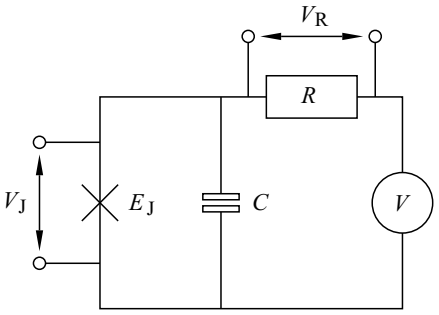

Fig. 2. Circuit modelling a real experimental set-up: a Josephson junction characterized by the Josephson energy E_J and capacitance C is coupled to a voltage source V via a resistor R. The voltage drops across the junction and the resistor are V_J and V_R, respectively.

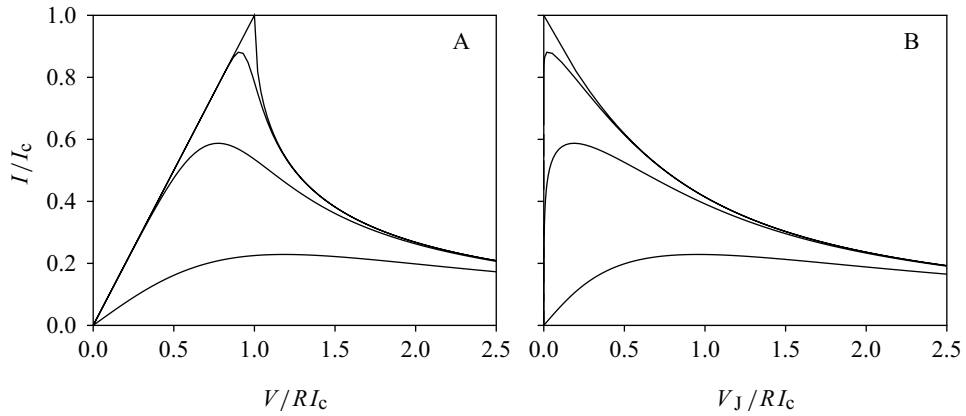

Fig. 3. A, Cooper pair current–voltage characteristics $I(V)$ [eqn (5)] in the overdamped phase diffusion regime for $\beta E_J = 1, 5, 50$, and ∞ from the lower to the upper curve and B, corresponding characteristics $I(V_J)$.

The term on the right-hand side represents the Nyquist noise with $\langle \delta V_R(t+\tau)\delta V_R(t)\rangle = (2R/\beta)\delta(\tau)$ for a resistor at inverse temperature $\beta = 1/k_B T$. Here, δV_R denotes the fluctuation of the voltage about its average value.

This problem has been solved by Ivanchenko and Zil'berman [6] in the overdamped limit where $2\pi^2\rho^2 E_J \ll E_c$. The stationary solution of the Fokker–Planck equation corresponding to eqn (4) can be expressed in terms of modified Bessel functions of complex order and yields the Cooper pair current [6]

$$\frac{I}{I_c} = \mathrm{Im}\left(\frac{I_{1-i\beta E_J v}(\beta E_J)}{I_{-i\beta E_J v}(\beta E_J)} \right) \tag{5}$$

as a function of the dimensionless applied voltage $v = V/RI_c$. While the supercurrent at zero voltage is destroyed by the fluctuations causing the phase diffusion, the current–voltage characteristics (5) display peaks at small but finite voltages as shown in Fig. 3A. With decreasing temperature the I–V curve (5) becomes closer to an ohmic line for voltages up to RI_c, while the peak in the I–V_J curve in Fig. 3B moves towards zero voltage.

We analyze the result (5) by considering the zero bias differential resistance

$$R_0 = \left.\frac{\partial V_J}{\partial I}\right|_{V_J=0} = \left.\frac{\partial V}{\partial I}\right|_{V=0} - R. \tag{6}$$

R_0 is defined with respect to the junction voltage V_J, and $1/R_0$ describes the slope at the origin in Fig. 3B. From eqn (5) one obtains

$$\frac{R_0}{R} = \frac{1}{I_0^2(\beta E_J) - 1}. \tag{7}$$

For $\beta E_J \gg 1$, the I–V curve is very close to $I = V/R$ with an exponentially small difference

$$\frac{R_0}{R} = 2\pi\beta E_J \exp(-2\beta E_J). \tag{8}$$

This shows that for temperatures much lower than the height of the periodic potential for φ in eqn (1), the dynamics of the phase is thermally activated.

On the other hand, for $\beta E_J \ll 1$, one finds in the overdamped limit

$$\frac{R_0}{R} = \frac{2}{(\beta E_J)^2}. \tag{9}$$

In this case, the I–V curve becomes

$$I = \frac{I_c^2}{2}\frac{RV}{V^2 + (2eR/\hbar\beta)^2} \tag{10}$$

which corresponds to a broad peak structure.

4. Coulomb blockade in Josephson junctions

We now turn to the case of ultrasmall tunnel junctions with spatial dimensions so small that $E_c \gg E_J$. Then the phase can no longer be treated as a quasiclassical variable, rather the charge on the junction capacitance will approximately follow classical statistics. As we have seen above, due to phase fluctuations, a supercurrent at zero voltage is no longer possible. However, a Cooper pair current may flow at finite voltages if the electromagnetic environment is able to absorb the energy $2eV$ gained by a Cooper pair tunneling through the junction. In contrast to Section 3, it is now necessary to introduce the external impedance on the quantum level. Due to its linearity the external impedance may be modeled by a possibly infinite number of LC oscillators. The corresponding Hamiltonian then reads

$$H_{\text{imp}} = \sum_{n=1}^{\infty} \frac{q_n^2}{2C_n} + \left(\frac{\hbar}{2e}\right)^2 \frac{1}{2L_n}(\varphi_R - \varphi_n)^2\Bigg]. \tag{11}$$

The external impedance in terms of the inductances L_n and capacitances C_n is given by

$$Z(\omega) = \left[\int_0^{\infty} dt e^{-i\omega t} \sum_{n=1}^{\infty} \frac{\cos(\omega_n t)}{L_n}\right]^{-1}, \tag{12}$$

where $\omega_n = (L_n C_n)^{-1/2}$. The coupling between the external impedance and the phase difference φ appears through the phase

$$\varphi_R = \frac{2e}{\hbar}\int_0^t dt'(V - V_J) = \frac{2e}{\hbar}Vt - \varphi. \tag{13}$$

This phase may formally be attributed to the resistance by making use of the Josephson relation (2).

Calculating the Cooper pair current from the Hamiltonian

$$H = H_J + H_{\text{imp}} \tag{14}$$

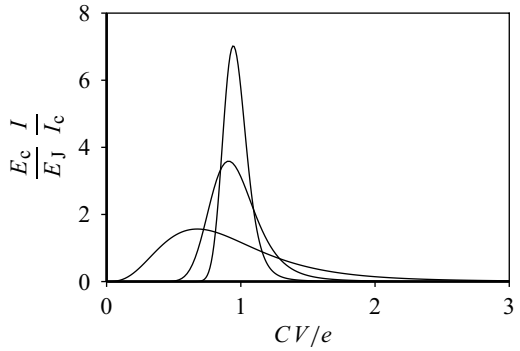

Fig. 4. Cooper pair current–voltage characteristics $I(V)$ in the Coulomb blockade regime at zero temperature. The peak is sharpening with increasing $\rho = 2, 20, 100$.

perturbatively to lowest order in E_J, one obtains [7, 8]

$$I = \frac{\pi e E_J^2}{\hbar}[P(2eV) - P(-2eV)]. \tag{15}$$

Here, $P(2eV)$ and $P(-2eV)$ are the probabilities that the energy $2eV$ of the tunneling Cooper pair is absorbed or provided by the environment, respectively. This probability depends on the external impedance and on temperature through [9]

$$P(E) = \frac{1}{2\pi\hbar}\int_{-\infty}^{+\infty} dt \exp\left[J(t) + \frac{i}{\hbar}Et\right] \tag{16}$$

with

$$J(t) = 2\int_{-\infty}^{\infty} \frac{d\omega}{\omega}\frac{\mathrm{Re}Z_t(\omega)}{R_Q}\frac{\mathrm{e}^{-i\omega t} - 1}{1 - \mathrm{e}^{-\beta\hbar\omega}}. \tag{17}$$

This expression contains the total impedance seen by the Josephson junction

$$Z_t(\omega) = \frac{1}{i\omega C + Z^{-1}(\omega)} \tag{18}$$

which is given by the external impedance in parallel with the capacitance.

For an ohmic environment $[Z(\omega) = R = \rho R_Q]$ the result (15) may be evaluated further. At zero temperature, one finds a zero bias anomaly given by $I \sim V^{2\rho-1}$. This shows that at $T = 0$ the perturbative result (15) is only valid for large $\rho > 1/2$ where the current remains small for all voltages. In this case the I–V curve displays a peak near voltages of order e/C as shown in Fig. 4. This can easily be understood from a simple Coulomb blockade picture. At $V = e/C$ the voltage gain $2eV$ just equals the charging energy E_c.

However, the experimentally relevant situation is an environment of low impedance ($\rho \ll 1$) [10]. On the one hand, it is difficult to fabricate large resistances at frequencies around $E_c/\hbar$, which typically is of the order of 10 GHz, and on the other hand the resistance should not be too large to avoid heating. Furthermore, since charging effects are washed out by thermal fluctuations, we are interested in the regime of low but finite temperatures $\beta E_c \gg 1$. To proceed for parameters in this range, we first note that the function $J(t)$ is equivalent to the position autocorrelation function of a free damped particle and can be evaluated in closed form for ohmic damping [11]. For long times, $J(t)$ describes diffusive behavior linear in time for finite temperatures and logarithmic in time at zero temperature. We therefore neglect exponentially decaying terms. This restricts us to low voltages which is the regime of interest. Assuming furthermore $\rho \ll \beta E_c$, in

accordance with the above considerations, we arrive at [12]

$$J(t) = -2\rho\left(\ln\left[\frac{\beta E_c}{\pi^2\rho}\sinh\left(\frac{\pi t}{\hbar\beta}\right)\right. \quad + \gamma + i\frac{\pi}{2}\mathrm{sign}(t)\right). \tag{19}$$

Here, $\gamma = 0.5772\ldots$ is the Euler constant. Inserting (19) into (16) and making use of (15) one finally obtains [12–14]

$$I = \frac{\pi}{2}I_c\frac{E_J}{E_c}\rho^{2\rho}\left(\frac{\beta E_c}{2\pi^2}\right)^{1-2\rho}\exp[-2\gamma\rho]\frac{\left|\Gamma\left(\rho - i\frac{\beta eV}{\pi}\right)\right|^2}{\Gamma(2\rho)}\sinh(\beta eV). \tag{20}$$

This perturbative result is only correct if the current is not too large, which may be the case for very small temperatures and very small damping. In fact, as noted above, at zero temperature one finds a divergence at low voltages. Therefore, the validity is restricted to not too low temperatures $\beta E_J \ll \rho$. Since $E_c \gg E_J$, this together with the upper bound on temperature [$\beta E_c \gg \rho$] still leaves a rather large range where (20) is applicable.

The current–voltage characteristics (20) is shown in Fig. 6 (see Section 5) as dashed line for $\beta E_J = 2$, $\rho = 0.04$ and $\beta E_c = 1$ and 10^5. It exhibits a peak at finite voltage which for small ρ is given by

$$V_{\max} = \frac{\pi\rho}{e\beta}(1 + 4\zeta(3)\rho^3 + \ldots). \tag{21}$$

Here $\zeta(3) = 1.202\ldots$ is a Riemann number. In the limit of small ρ, high temperatures and for $\beta\mathrm{eV} \ll 1$ one recovers the result of classical phase diffusion (10).

A *nonohmic environment* of practical interest is a finite LC transmission line terminated by an ohmic load resistance R_L [15, 16]. The transmission line is characterized by its resistance at infinite length $R_\infty = (L_0/C_0)^{1/2}$, where L_0 and C_0 are the specific inductance and capacitance per unit length. As a parameter describing the finite length ℓ of the transmission line we choose the $\lambda/4$-frequency $\omega_0 = (\pi/2)u/\ell$, where $u = (L_0C_0)^{-1/2}$ is the velocity of wavepropagation on the line.

Depending on the ratio between load resistance and resistance of the infinite transmission line, the environment behaves quite differently. For $R_L = R_\infty$ the impedance matching results in an ohmic impedance. On the other hand, for R_L very different from R_∞, the impedance displays sharp resonances. According to the above discussion, the properties of the external impedance should show up in the probability to absorb or emit energy, i.e. in $P(E)$, and therefore according to (15) in the Cooper pair current–voltage characteristics. This is indeed the case as can be seen from Fig. 5. There we show the zero-temperature Cooper pair current for $R_L/R_\infty = 0.1$ obtained from a direct numerical evaluation of eqns (15)–(17). The resonance peaks can be identified as single or multiple excitations of various transmission line modes [12]. The measurement of the Cooper pair current, thus, allows for a spectroscopy of the environmental modes.

5. Supercurrent peak: between the phase diffusion and Coulomb blockade regimes

So far, we have discussed the behavior of a Josephson junction in the classical overdamped limit (Section 3) and in the quantum regime for charging energies much larger than the Josephson coupling energy (Section 4). We now want to bridge the gap between these two limits by extending the perturbation theory presented in the previous section to infinite order in E_J.

The summation of the perturbation series in E_J is only possible for an appropriate choice of the parameter regime. Motivated by the above discussion, we will continue to consider the overdamped regime where $\omega_R = 1/RC$ is much larger than the Josephson frequency $\omega_J = (2e/\hbar)RI_c$. This is identical to the condition $2\pi^2\rho^2E_J \ll E_c$ given in Section 3. In addition, the correlation function $J(t)$ contains a thermal frequency scale given by $\nu = 2\pi/\hbar\beta$ as can be seen from the last denominator in eqn (17). In the following we assume

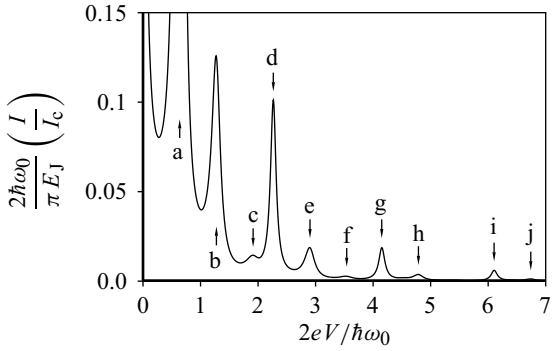

Fig. 5. Cooper pair current–voltage characteristic for an ultrasmall tunnel junction coupled to a finite transmission line with $R_L/R_Q = 0.01$, $R_L/R_\infty = 0.1$, and $\omega_0 R_\infty C = 1$ at zero temperature. The peaks correspond to excitations denoted by $(N_1 N_2 N_3 N_4)$, where N_k is the number of quanta of the k-th mode excited. a, (1000), b, (2000), c, (3000), d, (0100), e, (1100), f, (2100), g, (0010), h, (1010), i, (0001), j, (1001).

that $\omega_J \ll \nu$, so that we may neglect terms exponentially decaying in time with ν or faster. This results in the approximation

$$J(t) = -2\rho\left[\frac{\pi}{\hbar\beta}|t| + S + i\frac{\pi}{2}\mathrm{sign}(t)\right] \tag{22}$$

valid for sufficiently high temperatures where $\rho\beta E_J \ll 1$. Further, we have introduced the abbreviation

$$S = \gamma + \frac{\pi^2\rho}{\beta E_c} + \psi\left(\frac{\beta E_c}{2\pi^2\rho}\right), \tag{23}$$

where $\psi(x)$ denotes the logarithmic derivative of the gamma function.

For the correlation function (22) the Cooper pair current can be evaluated exactly and expressed in terms of a continued fraction [17]

$$I = I_c \mathrm{Re}\left[\frac{\sin(\pi\rho)}{2\pi\rho}\frac{\exp(-2\rho S)}{v + i/\beta E_J}\cfrac{1}{1+\cfrac{b_1}{1+\cfrac{b_2}{1+\ldots}}}\right] \tag{24}$$

with coefficients

$$b_n = \left(\frac{\beta E_J}{2\pi\rho}\right)^2 \frac{\sin(\pi\rho n)\sin(\pi\rho(n+1))\exp(-2\rho S)}{n(n+1)(n - iv\beta E_J)(n+1-iv\beta E_J)}. \tag{25}$$

Since the continued fraction converges rapidly, we may linearize the sine functions appearing in eqn (25) for sufficiently small ρ. Then, the continued fraction may be evaluated with the help of a matrix recursion and one finds [17]

$$I = \frac{2e}{\hbar}E_J^* \mathrm{Im}\left(\frac{I_{1-i\beta eV/\pi\rho}(\beta E_J^*)}{I_{-i\beta eV/\pi\rho}(\beta E_J^*)}\right) \tag{26}$$

with an effective Josephson energy

$$E_J^* = E_J \exp(-\rho[\psi(1+\hbar\beta\omega_R/2\pi) + \gamma]). \tag{27}$$

Here we have rewritten the quantity S defined in eqn (23) in terms of the frequency ω_R and have neglected

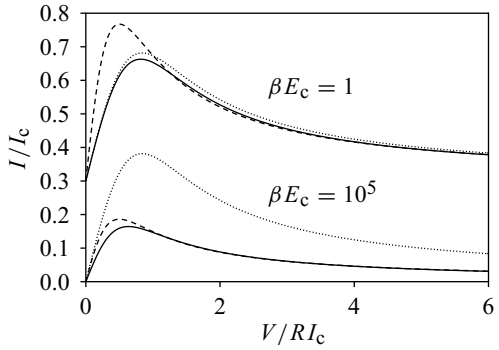

Fig. 6. The current–voltage characteristic of a Josephson junction with Josephson energy $\beta E_J = 2$ is shown for charging energies $\beta E_c = 1$ and 10^5 and external resistance $\rho = 0.04$. The full line corresponds to our result (24) while the dotted line gives the standard Ivanchenko–Zil'berman result (5) and the dashed line depicts the prediction (20) for Coulomb blockade. The two sets of current–voltage characteristics are vertically shifted with respect to each other by $I/I_c = 0.3$ for sake of clarity.

a term $\pi\rho/\hbar\beta\omega_R \ll 1$ in the overdamped limit considered. Even though ρ has to be small for the expression (27) to hold, the correction to the bare Josephson energy may be substantial because for low temperatures the ψ function grows logarithmically and may become large. On the other hand, in the classical limit where $\hbar \to 0$ and $e \to 0$ such that the flux quantum $h/2e$ remains constant, the effective Josephson energy E_J^* coincides with the bare Josephson energy E_J. We thus recover in the classical overdamped limit the result (5).

In Fig. 6 we show how the result (26) bridges between the phase diffusion result (5) shown as a dotted line and the Coulomb blockade result (20) depicted as a dashed line. The current–voltage characteristics have been calculated for $\beta E_J = 2$ and $\rho = 0.04$. For large βE_c, where charging effects should be important, one obtains very good agreement with the Coulomb blockade result. With decreasing βE_c the current–voltage characteristics evolve differently and a crossover to the Ivanchenko–Zil'berman result is found.

6. Conclusions

We have studied the current–voltage characteristics of mesoscopic Josephson junctions focusing on the modifications of the supercurrent as the junction parameters change. We have not discussed here the effect of the charging energy on quasiparticle tunneling relevant at higher applied voltages only [18]. As the charging energy E_c grows relative to the Josephson energy E_J, the supercurrent of the classical Josephson effect was shown to evolve gradually into a supercurrent peak caused by incoherent Cooper pair tunneling. In the Coulomb blockade regime two types of structures may appear for small junctions with $E_J \ll E_c$ embedded in a standard low impedance environment. The first structure, a peak at low voltages has recently been seen in experiments on lithographically fabricated junctions [15, 16] as well as break junctions [19]. The second structure, peaks in the current–voltage characteristics due to resonances in the environmental impedance have also been seen in experiments [15, 16] with a well-defined environment consisting of two transmission line segments allowing for a quantitative test of the theoretical predictions and good agreement was found. Although detailed experimental studies of the region between the phase diffusion and Coulomb blockade limits are absent, recent work [20] indicates quantum effects in qualitative accord with the predictions made.

Acknowledgements—We would like to thank M. H. Devoret, D. Esteve, and C. Urbina for stimulating discussions. One of us (HG) was supported by the Deutsche Akademischer Austauschdienst (DAAD), while support for the other author (GLI) during a stay at the Centre d'Etudes de Saclay was provided by the Volkswagenstiftung.

References

[1] A. Barone and G. Paternò, *Physics and Applications of the Josephson Effect* (Wiley, New York, 1982).
[2] M. Tinkham, *Introduction to Superconductivity* (McGraw-Hill, New York, 1996) 2nd edn.
[3] G. Schön and A. D. Zaikin, Phys. Rep. **198**, 237 (1990).
[4] *Single Charge Tunneling*, NATO ASI Series B, Vol. 294, edited by H. Grabert and M. H. Devoret (Plenum, New York, 1991).
[5] R. L. Kautz and J. M. Martinis, Phys. Rev. **B42**, 9903 (1990).
[6] Yu. M. Ivanchenko and L. A. Zil'berman, Zh. Eksp. Teor. Fiz. **55**, 2395 (1968) [Sov. Phys. JETP **28**, 1272 (1969)].
[7] D. V. Averin, Yu. V. Nazarov, and A. A. Odintsov, Physica **B165&166**, 945 (1990).
[8] G.-L. Ingold and Yu. V. Nazarov, in Ref. [4].
[9] M. H. Devoret, D. Esteve, H. Grabert, G.-L. Ingold, H. Pothier, and C. Urbina, Phys. Rev. Lett. **64**, 1824 (1990).
[10] M. H. Devoret and H. Grabert, in Ref. [4].
[11] H. Grabert, P. Schramm, and G.-L. Ingold, Phys. Rep. **168**, 115 (1988).
[12] G.-L. Ingold, H. Grabert, and U. Eberhardt, Phys. Rev. **B50**, 395 (1994).
[13] H. Grabert and G.-L. Ingold, *Computations for the Nano-Scale*, NATO ASI Series E, Vol. 240, edited by P. E. Blöchl, C. Joachim, and A. J. Fisher (Kluwer, Dordrecht, 1993).
[14] G.-L. Ingold and H. Grabert, Physica **B194–196**, 1025 (1994).
[15] T. Holst, D. Esteve, C. Urbina, and M. H. Devoret, Physica **B203**, 397 (1994).
[16] T. Holst, D. Esteve, C. Urbina, and M. H. Devoret, Phys. Rev. Lett. **73**, 3455 (1994).
[17] H. Grabert, G.-L. Ingold, and B. Paul, Europhys. Lett. **44**, 360 (1998).
[18] G. Falci, V. Bubanja, and G. Schön, Europhys. Lett. **16**, 109 (1991).
[19] C. J. Muller and R. de Bruyn Ouboter, Physica **B194–196**, 1043 (1994).
[20] D. Vion, M. Götz, P. Joyez, D. Esteve, and M. H. Devoret, Phys. Rev. Lett. **77**, 3435 (1996).